

Physics potentials of large liquid detectors

Liquid Argon (GLACIER), Liquid Scintillator (LENA) and Water Čerenkov(MEMPHYS)

J-E Campagne^a, A. Bueno^b, L. Oberauer^c
List of authors to be completed.

Abstract

A brief Status Report on the Physics Potential of the projects.

Contribution to the European Funding demand

1 Introduction

The pioneer Water Čerenkov detectors (IMB, Kamiokande) were built to look for Nucleon Decay, a prediction of Grand Unified Theories. In fact, the Neutrino physics has been the bread and butter since the beginning of operation of such detectors. Just to remind the glorious past: first detection of a Super Novae neutrino burst, Solar and Atmospheric anomalies discovery that was explained as mass & mixing of the neutrinos, the latter being confirmed by the first long base line neutrino beam.

The proposed detectors (GLACIER, LENA, MEMPHYS) using different techniques will push the discovery frontiers on many domains: Proton Decay, Supernova neutrino (burst and diffuse past explosion), Solar and Atmospheric neutrinos, Geo-neutrinos, long baseline neutrinos, indirect dark matter search...

2 Brief detector description

2.1 Liquid Argon TPC

GLACIER (Fig. 1) is the foreseen extrapolation up to 100 kT of a Liquid Argon Time Projecting Chamber [1]. A summary of parameters are listed in Table 1. The detector can be mechanically subdivided into two parts: (1) the liquid argon tanker and (2) the inner detector instrumentation. For simplicity, we assume at this stage that the two aspects can be decoupled.

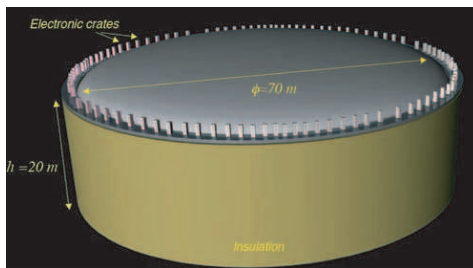


Figure 1: An artistic view of a 100 kton single tanker liquid argon detector. The electronic crates are located at the top of the dewar.

The basic design parameters can be summarized as follows:

1. Single 100 kton “boiling” cryogenic tanker with Argon refrigeration (in particular, the cooling is done directly with Argon, e.g. without nitrogen)
2. Charge imaging + scintillation + Čerenkov light readout for complete event information
3. Charge amplification to allow for extremely long drifts: the detector is running in bi-phase mode. In order to allow for long drift ($\approx 20\text{ m}$), we consider charge

attenuation along drift and compensate this effect with charge amplification near anodes located in gas phase.

4. Absence of magnetic field

Dewar	$\Phi \approx 70$ m, height ≈ 20 m, passive perlite insulated, heat input ≈ 5 W/m ²
Argon Storage	Boiling argon, low pressure (< 100 mb over-pressure)
Argon total volume	73118 m ³ (height = 19 m), ratio area/volume $\approx 15\%$
Argon total mass	102365 TONS
Hydrostatic pressure at bottom	≈ 3 atm
Inner detector dimensions	Disc $\Phi \approx 70$ m located in gas phase above liquid phase
Electron drift in liquid	20 m maximum drift, HV= 2MV for E=1 kV/cm, $v_d \approx 2$ mm/ μ s, max drift time ≈ 10 ms
Charge readout views	2 independent perpendicular views, 3 mm pitch, in gas phase (electron extraction) with charge amplification
Charge readout channels	≈ 100000
Readout electronics	100 racks on top of dewar (1000 channels per crate)
Scintillation light readout	Yes (also for triggering), 1000 immersed 8" PMT with WLS (TPB)
Visible light readout	Yes (Cerenkov light), 27000 immersed 8" PMTs or 20% coverage, single photon counting capability

Table 1: Summary parameters of the 100 kton liquid Argon detector

The inner detector instrumentation is made of: A cathode, located near the bottom of the tanker, set at $-2MV$ that creates a drift electric field of 1 kV/cm over the distance of 20 m. In this field configuration ionization electrons are moving upwards while ions are going downward. The electric field is delimited on the sides of the tanker by a series of ring electrodes (race-tracks) put at the appropriate voltages (voltage divider). The breakdown voltage of liquid argon is such that a distance of about 50 cm to the grounded tanker volume is electrically safe. For the high voltage we consider two solutions: (1) either the HV is brought inside the dewar through an appropriate custom-made HV feed-through or (2) a voltage multiplier could be installed inside the cold volume.

The relevant parameters of the charge readout are summarized in Table 2. The tanker contains both liquid and gas argon phases at equilibrium. Since purity is a concern for very long drifts of the order of 20 meters, we think that the inner

detector should be operated in bi-phase mode, namely drift electrons produced in the liquid phase are extracted from the liquid into the gas phase with the help of an appropriate electric field. Our measurements show that the threshold for 100% efficient extraction is about 3 kV/cm. Hence, just below and above the liquid two grids define the appropriate liquid extraction field. In addition to charge readout, we envision to locate PMTs around the tanker. Scintillation and Cerenkov light can be readout essentially independently. One can profit from the ICARUS R&D which has shown that PMTs immersed directly in the liquid Argon is possible[2]. One is using commercial Electron Tubes 8" PMTs with a photocathode for cold operation and a standard glass window. In order to be sensitive to DUV scintillation, the PMT are coated with a wavelength shifter (Tetraphenyl-Butadiene). Summarizing about 1000 immersed phototubes with WLS would be used to identify the (isotropic and bright) scintillation light. While about 27000 immersed 8"-phototubes without WLS would provide a 20% coverage of the surface of the detector. As already mentioned, these latter should have single photon counting capabilities in order to count the number of Cerenkov photons.

Electron drift in liquid	20 m maximum drift, HV=2 MV for E=1kV/cm, $v_d \simeq 2mm/\mu s$, max drift time $t_{max} \simeq 10$ ms
Charge readout views	two independent perpendicular views, 3 mm pitch
Maximum charge diffusion	$\sigma_D \simeq 2.8mm$ ($\sqrt{2Dt_{max}}$ for $D = 4cm^2/s$)
Maximum charge attenuation	$e^{-t_{max}/\tau} \simeq 1/150$ for $\tau = 2$ ms electron life-time
Needed charge amplification	10^2 to 10^3
Methods for amplification	Extraction to and amplification in gas phase
Possible solutions	Thin wires+pad readout, GEM, LEM, ...

Table 2: Parameters of the charge readout

2.2 Liquid Scintillator

LENA (Fig. ??) [?] is the foreseen extrapolation up to 50 kT ($\phi = 30$ m, *Leangth* = 100 m) of PXE Liquid Scintillator surrounded by a water active veto shielding. **To be completed for LENA**

2.3 Water Čerenkov

MEMPHYS (Fig. 2) [3] is the foreseen extrapolation up to 730 kT Water Čerenkov. The detector is a collection of up to 5 shafts, and 3 are enough for 500 kt fiducial mass which is used hereafter. Each shaft is 65 m in diameter and 65 m height for the total water container dimensions, and this represent an extrapolation of a factor 4

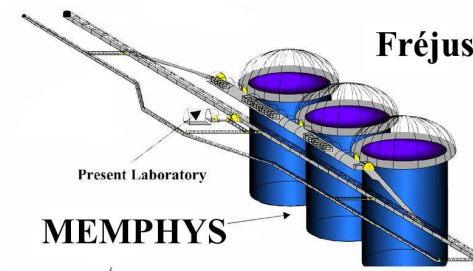


Figure 2: Sketch of the MEMPHYS detector under the Fréjus mountain (Europe).

with respect to the Super-Kamiokande running detector. The PMT surface defined as 2 m inside the water container is covered by about 81,000 12" PMTs to reach a 30% surface coverage equivalent to a 40% coverage with 20" PMTs. The fiducial volume is defined by an additional conservative guard of 2 m. The outer volume between the PMT surface and the water vessel is instrumented with 8" PMTs. If not contrary mentionned, the Super-Kamiokande analysis (efficiency, background reduction) [8] is used to compute the physics potential of such a detector. In the US and in Japan, there are two competitors to MEMPHYS, namely UNO and Hyper-Kamiokande. These projects are similar in many respects and the hereafter presented physics potential may be foreseen also for those detectors. Currently, there is a very interesting R&D activity concerning the possibility to introduce Gadolinium salt (GdCl_3) inside the 1 kT Water Čerenkov prototype of the K2K experiment. The physics goal is to decrease the background in many physics channels by tagging the neutron produced in the inverse beta decay interaction of $\bar{\nu}_e$ on free proton. For instance, 100 tons of GdCl_3 in SuperKamiokande would yield more than 90% neutron captures on Gd [7].

3 Detector Performances

3.1 Proton decay sensitivity

version 0 by JEC 6/3/06

update Introduction by Pavel F. Perez 8/3/06

update by A. Bueno 23/3/06

For all relevant aspects of the proton stability in grand unified theories, in strings and in branes see reference [9].

Since proton decay is the most dramatic prediction coming from theories where the matter is unified, we hope to test those scenarios at future experiments. For this reason, a theoretical upper bound on the lifetime of the proton is very important to know about the possibilities of future experiments.

Recently a model-independent upper bound on the total proton decay lifetime has been pointed out [10]:

$$\tau_p^{upper} = \left\{ \begin{array}{ll} 6.0 \times 10^{39} & \text{(Majorana case)} \\ 2.8 \times 10^{37} & \text{(Dirac case)} \end{array} \right\} \times \frac{(M_X/10^{16} \text{GeV})^4}{\alpha_{GUT}^2} \times \left(\frac{0.003 \text{GeV}^3}{\alpha} \right)^2 \text{ yrs} \quad (1)$$

where M_X is the mass of the superheavy gauge bosons. The parameter $\alpha_{GUT} = g_{GUT}^2/4\pi$, where g_{GUT} is the gauge coupling at the grand unified scale. α is the matrix element. See Figures (3) and (4) for the present parameter space allowed by the experiments.

Most of the models (Supersymmetric or non-Supersymmetric) predict a lifetime τ_p below those upper bounds 10^{33-37} years, which are very interesting since it is the possible range of the proposed detectors.

In order to have an idea of the proton decay predictions, let us list in Tab.3 the results in different models.

Model	Decay modes	Prediction	References
Georgi-Glashow model	-	ruled out	[11]
Minimal realistic non-SUSY $SU(5)$	all channels	$\tau_p^{upper} = 1.4 \times 10^{36}$	[12]
Two Step Non-SUSY $SO(10)$	$p \rightarrow e^+ \pi^0$	$\approx 10^{33-38}$	[13]
Minimal SUSY $SU(5)$	$p \rightarrow \bar{\nu} K^+$	$\approx 10^{32-34}$	[14]
SUSY $SO(10)$ with 10_H , and 126_H	$p \rightarrow \bar{\nu} K^+$	$\approx 10^{33-36}$	[15]
M-Theory(G_2)	$p \rightarrow e^+ \pi^0$	$\approx 10^{33-37}$	[16]

Table 3: Summary of some recent predictions on proton partial lifetimes.

No specific simulation for MEMPHYS has been carried out yet. We therefore rely on the study done by UNO, adapting the results to MEMPHYS (which has an overall better coverage) when possible.

Due to its excellent imaging and energy resolution, GLACIER has the potentiality to discover nucleon decay in an essentially background-free environment. To understand the potential background contamination for this kind of search, we have carried out a detailed simulation of nucleon decays in Argon, i.e. including final state nuclear effects. This is vital since (1) they change the exclusive final state configuration and (2) they introduce a distortion of the event kinematics. Atmospheric neutrino and cosmic muon induced backgrounds have been fully simulated as well.

General remarks for LENA

3.1.1 $p \rightarrow e^+ \pi^0$

Following UNO study, the detection efficiency of $p \rightarrow e^+ \pi^0$ (3 showering rings event) is $\epsilon = 43\%$ for a 20 inch-PMT coverage of 40% or its equivalent, as envisioned for MEMPHYS. The corresponding estimated atmospheric neutrino induced background is at the level of 2.25 events/Mt.yr. From these efficiencies and background levels, proton decay sensitivity as a function of detector exposure can be estimated (see Fig. 5). A 10^{35} years partial lifetime (τ_p/B) could be reached at the 90% CL for a 5 Mt.yr exposure (10 yrs) with MEMPHYS (similar to case A in figure 5). Beyond that exposure, tighter cuts may be envisaged to further reduce the atmospheric neutrino background to 0.15 events/Mt.yr, by selecting quasi exclusively the free proton decays.

The positron and the two photons issued from the π^0 gives clear events in the GLACIER detector. We find that the π^0 is absorbed by the nucleus $\sim 45\%$ of the times. Assuming a perfect particle and track identification, one may expect a 45% efficiency and a background level of 1 event/Mt.y. So, for a 1 Mt.yr (10 yrs) exposure with GLACIER one reaches $\tau_p/B > 0.5 \cdot 10^{35}$ yrs at 90% CL (see Fig. 7).

LENA part to be added

3.1.2 $p \rightarrow \bar{\nu} K^+$

Since the K^+ momentum (360 MeV) is below the water Čerenkov threshold in MEMPHYS (570 MeV), this channel is much more favorable for LENA and GLACIER.

LENA use the pulse shape analysis (rise time) to discriminate the kaon production then decay 18 ns later, from the atmospheric neutrino kaon production and the atmospheric neutrino charged current production of muon and charged pion. The signal efficiency is expected to be 65% keeping the background below 1 event/Mt.y. Then, one can reach $\tau_p/B > 4 \cdot 10^{34}$ yrs (90% CL) in 0.5 Mt.yr exposure (10 yrs). To be completed by LENA

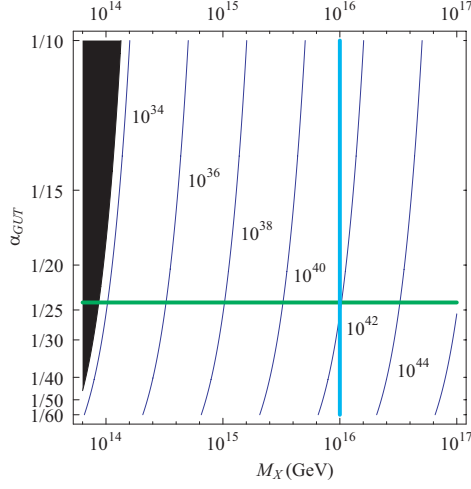


Figure 3: Isoplot for the upper bounds on the total proton lifetime in years in the Majorana neutrino case in the M_X - α_{GUT} plane. The value of the unifying coupling constant is varied from $1/60$ to $1/10$. The conventional values for M_X and α_{GUT} in SUSY GUTs are marked in thick lines. Experimentally excluded region is given in black [10].

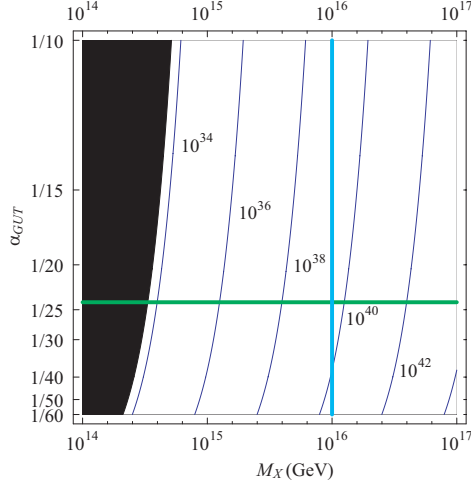


Figure 4: Isoplot for the upper bounds on the total proton lifetime in years in the Dirac neutrino case in the M_X - α_{GUT} plane. The value of the unifying coupling constant is varied from $1/60$ to $1/10$. The conventional values for M_X and α_{GUT} in SUSY GUTs are marked in thick lines. Experimentally excluded region is given in black [10].

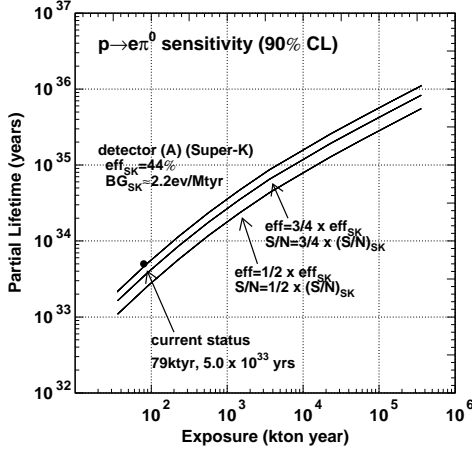


Figure 5: Sensitivity for $e^+\pi^0$ proton decay lifetime, as determined by UNO [6]. MEMPHYS corresponds to case (A).

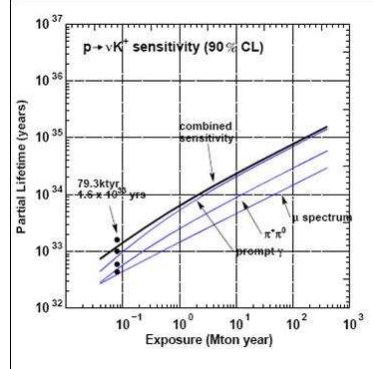


Figure 6: Expected sensitivity on νK^+ proton decay as a function of MEMPHYS exposure [6] (see text for details).

GLACIER uses dE/dx versus range as discriminating variable in a Neural Net to obtain the particle identity. We expect less than 1% of kaons mis-identified as protons. In this channel, the selection efficiency is high (97%) for a low background < 1 event/Mt.y. In case of absence of signal, we expect to reach $\tau_p/B > 1.1 \cdot 10^{35}$ yrs at 90% CL for 1 Mt.y (10 years) exposure (see Fig. 7).

For the MEMPHYS detector, one should rely on the detection of the decay products of the kaon: a 256 MeV/c muon and its decay electron (type I) or a 205 MeV/c π^+ and π^0 (type II), with the possibility of a delayed (12 ns) coincidence with the 6 MeV ^{15}N de-excitation prompt γ (Type III). Using the imaging and timing capability of Super-Kamiokande, the efficiency for the reconstruction of $p \rightarrow \bar{\nu} K^+$ is $\epsilon = 33\%$ (I), 6.8% (II) and 8.8% (III), and the background is at 2100, 22 and 6 events/Mt.yr level. For the prompt γ method, the background is dominated by mis-reconstruction. As stated by UNO, there are good reasons to believe that this background can be lowered by at least a factor 2 corresponding to the atmospheric neutrino interaction $\nu p \rightarrow \nu \Lambda K^+$. In these conditions, and using Super-Kamiokande performances, a 5 Mt.yr MEMPHYS exposure would allow to reach $\tau_p/B > 2 \cdot 10^{34}$ yrs partial (see Fig. 6).

3.1.3 Comparison between the detectors

Preliminary comparisons have been done between the detectors (Tab. 4). For the $e^+\pi^0$ channel, the Čerenkov detector gets a better limit due to their higher mass. However it should be noted that GLACIER, although five times smaller in mass

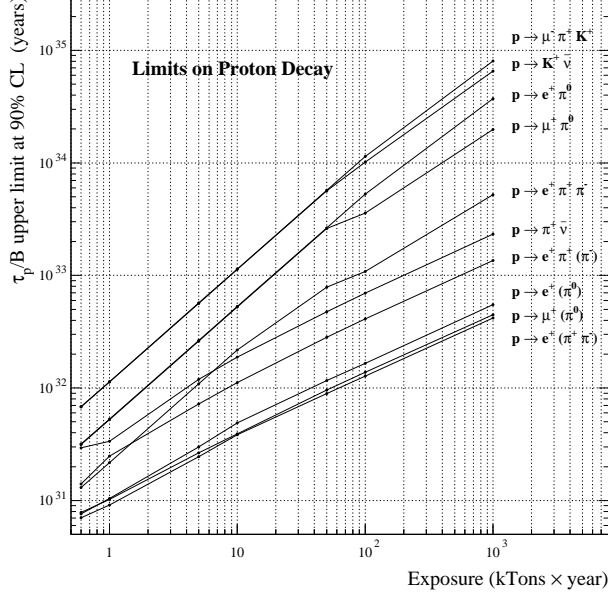


Figure 7: Expected proton decay lifetime limits (τ/B at 90% C.L.) as a function of exposure for GLACIER.

than MEMPHYS, gets an expected limit that is only a factor two smaller. Liquid argon TPCs and liquid scintillator detectors get better results for the $\bar{\nu}K^+$ channel, due to their higher detection efficiency. The two techniques look therefore quite complementary and the EU Network would investigate deeper the pro and cons of each techniques with other channels not yet investigated by the present study but interesting too as $e^+(\mu^+) + \gamma$ and neutron decays.

3.2 Supernova neutrinos

Version 0 by JEC 28/2/06: sort of summary of A. Mirizzi talk 16/2/06.

update by A. Bueno 23/3/06

update by A. Mirizzi 9/4/06

A supernova (SN) neutrino detection represents one of the next frontiers of neutrino astrophysics. It will provide invaluable information on the astrophysics of the core-collapse explosion phenomenon and on the neutrino mixing parameters. In particular, neutrino flavor transitions in the SN envelope are sensitive to the value of θ_{13} and on the type of mass hierarchy, and the detection of SN neutrino spectra at Earth can significantly contribute to sharpen our understanding of these unknown neutrino

	GLACIER	LENA	MEMPHYS
$e^+\pi^0$			
$\epsilon(\%)/\text{Bkgd}(\text{Mt.y})$	45/1	-	43/2.25
τ_p/B (90% CL, 10 yrs)	0.5×10^{35}	-	1.0×10^{35}
$\bar{\nu}K^+$			
$\epsilon(\%)/\text{Bkgd}(\text{Mt.y})$	97/1	65/1	8.8/3
τ_p/B (90% CL, 10 yrs)	1.1×10^{35}	0.4×10^{35}	0.2×10^{35}

Table 4: Summary

parameters. On the other hand, a detailed measurement of the neutrino signal from a galactic SN could yield important clues on the SN explosion mechanism.

3.2.1 SN neutrino emission and oscillations

A core-collapse supernova marks the evolutionary end of a massive star ($M \gtrsim 8 M_\odot$) which becomes inevitably instable at the end of its life: it collapses and ejects its outer mantle in a shock-wave driven explosion. The collapse to a neutron star ($M \simeq M_\odot$, $R \simeq 10$ km) liberates a gravitational binding energy, $E_B \approx 3 \times 10^{53}$ erg, released at $\sim 99\%$ into (anti)neutrinos of all the flavors, and only at $\sim 1\%$ into the kinetic energy of the explosion. Therefore, a core-collapse SN represents one of the most powerful sources of (anti)neutrinos in the Universe.

In general, numerical simulations of supernova explosions provide the original neutrino spectra in energy and time F_ν^0 . Such initial distributions are in general modified by flavor transitions in SN envelope, in vacuum (and eventually in Earth matter)

$$F_\nu^0 \longrightarrow F_\nu \ , \quad (2)$$

and must be convoluted with the differential interaction cross section σ_e for electron or positron production, as well as with the detector resolution function R_e , and the efficiency ε , in order to finally get observable event rates ,

$$N_e = F_\nu \otimes \sigma_e \otimes R_e \otimes \varepsilon \ . \quad (3)$$

Regarding the initial neutrino distributions F_ν^0 , a SN collapsing core is roughly a black-body source of thermal neutrinos, emitted on a timescale of ~ 10 s. Energy spectra parametrization are typically cast in the form of quasi-thermal distributions, with typical average energies: $\langle E_{\nu_e} \rangle = 9 - 12$ MeV, $\langle E_{\bar{\nu}_e} \rangle = 14 - 17$ MeV, $\langle E_{\nu_x} \rangle = 18 - 22$ MeV, where ν_x indicates any non-electron flavor.

The oscillated neutrino fluxes arriving at Earth may be written in terms of the

Mass Hierarchy	$\sin^2 \theta_{13}$	p	\bar{p}
Normal	$\gtrsim 10^{-3}$	0	$\cos^2 \theta_{12}$
Inverted	$\gtrsim 10^{-3}$	$\sin^2 \theta_{12}$	0
Any	$\gtrsim 10^{-5}$	$\sin^2 \theta_{12}$	$\cos^2 \theta_{12}$

Table 5: Values of the p and \bar{p} parameters used in Eq. (4)–(6) in different scenario of mass hierarchy and $\sin^2 \theta_{13}$.

energy-dependent “survival probability” p (\bar{p}) for neutrinos (antineutrinos) as [17]

$$F_{\nu_e} = pF_{\nu_e}^0 + (1-p)F_{\nu_x}^0, \quad (4)$$

$$F_{\bar{\nu}_e} = \bar{p}F_{\bar{\nu}_e}^0 + (1-\bar{p})F_{\nu_x}^0, \quad (5)$$

$$4F_{\nu_x} = (1-p)F_{\nu_e}^0 + (1-\bar{p})F_{\bar{\nu}_e}^0 + (2+p+\bar{p})F_{\nu_x}^0, \quad (6)$$

where ν_x stands for either ν_μ or ν_τ . The probabilities p and \bar{p} crucially depend on the neutrino mass hierarchy and on the unknown value of the mixing angle θ_{13} as shown in Table 5.

3.2.2 SN neutrino detection in MEMPHYS, GLACIER, LENA

Galactic core-collapse supernovae are rare, perhaps a few per century. Up to now, supernova neutrinos have been measured only once during SN 1987A explosion in the Large Magellanic Cloud ($d = 50$ kpc). Due to the relatively small masses of the detectors operative at that time, only few events were detected (11 in Kamiokande [18, 19] and 8 in IMB [20]). The three proposed large-volume neutrino detectors with a broad range of science goals might guarantee continuous exposure for several decades, so that a high-statistics supernova neutrino signal may eventually be observed.

Expected number of events for GLACIER, MEMPHYS and LENA are reported in Table 6, for a typical galactic SN distance of 10 kpc. In the upper panel it is reported the total number of events, while the lower part refers to the ν_e signal detected during the prompt neutronization burst, with a duration of ~ 25 ms, just after the core bounce.

One can realize that $\bar{\nu}_e$ detection by Inverse β Decay is the golden channel for MEMPHYS and LENA, while GLACIER has a unique opportunity to see the ν_e by charged current interactions on ^{40}Ar with a very low threshold. This detection complementarity is of great interest and would assure a unique way to probe SN explosion mechanism as well as neutrino intrinsic properties. Moreover, the huge statistics would allow spectral studies in time and in energy domain.

We stress that it will be difficult to establish SN neutrino oscillation effects solely on the basis of a $\bar{\nu}_e$ or ν_e “spectral hardening” relative to theoretical expectations. Therefore, in the recent literature the importance of model-independent signatures has been emphasized. Here we focus mainly on the signatures associated to: the

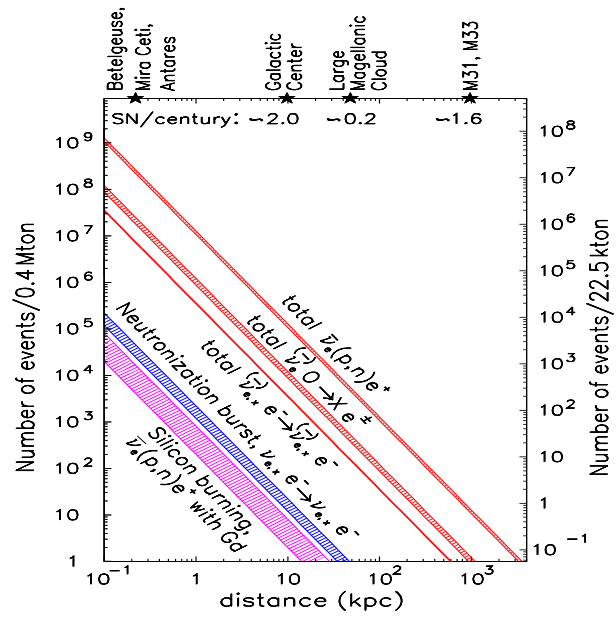


Figure 8: *The number of events in a 400 kt water Čerenkov detector (left scale) and in SK (right scale) in all channels and in the individual detection channels as a function of distance for a supernova explosion [26].*

MEMPHYS		LENA		GLACIER	
Interaction	Rates	Interaction	Rates	Interaction	Rates
$\bar{\nu}_e$ I β D	2×10^5	$\bar{\nu}_e$ I β D	9×10^3	$\nu_e^{CC}(^{40}\text{Ar}, ^{40}\text{K}^*)$	2.5×10^4
$\nu_e^{(-)CC}(^{16}\text{O}, X)$	10^4	ν_x pES	7×10^3	$\nu_x^{NC}(^{40}\text{Ar}^*)$	3.0×10^4
ν_x eES	10^3	$\nu_x^{NC}(^{12}\text{C}^*)$	3×10^3	ν_x eES	10^3
		ν_x eES	600	$\bar{\nu}_e^{CC}(^{40}\text{Ar}, ^{40}\text{Cl}^*)$	540
		$\bar{\nu}_e^{CC}(^{12}\text{C}, ^{12}\text{B}^{\beta+})$	500		
		$\nu_e^{CC}(^{12}\text{C}, ^{12}\text{N}^{\beta-})$	85		
Neutronization Burst rates					
MEMPHYS	60	ν_e eES			
LENA	10 ???	$\nu_e^{CC}(^{12}\text{C}, ^{12}\text{N}^{\beta-})$			
GLACIER	380	$\nu_x^{NC}(^{40}\text{Ar}^*)$			

Table 6: Summary of the expected neutrino interaction rates in the different detectors for a $8M_\odot$ SN located at 10 kpc (Galactic center). The following notations have been used: I β D, eES and pES stands for Inverse β Decay, electron and proton Elastic Scattering, respectively. The final state nuclei are generally unstable and decay either radiatively (notation *), or by β^-/β^+ weak interaction (notation β^-, β^+).

prompt ν_e neutronization burst, the shock-wave propagation, the Earth matter crossing.

The analysis of the time structure of the SN signal during the first few tens of milliseconds after the core bounce can provide a clean indication if the full ν_e burst is present or absent and therefore allows one to distinguish between different mixing scenarios as indicated by the third column of Table 7. For example, if the mass ordering is normal and the θ_{13} is large, the ν_e burst will fully oscillate into ν_x . If θ_{13} is measured in the laboratory to be large, for example by one of the forthcoming reactor experiments, then one may distinguish between the normal and inverted mass ordering.

As discussed, MEMPHYS is mostly sensitive to the I β D, although the ν_e channel can be measured by the elastic scattering reaction $\nu_x + e^- \rightarrow e^- + \nu_x$ [21]. Of course, the identification of the neutronization burst is cleanest with a detector using the charged-current absorption of ν_e neutrinos, like GLACIER. Using its unique features to look at ν_e CC it is possible to probe oscillation physics during the early stage of the SN explosion, and using the NC it is possible to decouple the SN mechanism from the oscillation physics [22, 23].

A few seconds after core bounce, the SN shock wave will pass the density region in the stellar envelope relevant for oscillation matter effects, causing a transient modification of the survival probability and thus a time-dependent signature in the neutrino signal [24, 25]. It would show a characteristic dip when the shock wave

passes [26], or a double-dip feature if a reverse shock occurs [27]. The detectability of such a signature has been studied in a Megaton Water Čerenkov detector like MEMPHYS by the $I\beta D$ [26], and in a Large liquid Argon detector like GLACIER by Ar CC interactions [28]. The shock wave effects would be certainly visible also in a large volume scintillator like LENA. Of course, apart from identifying the neutrino mixing scenario, such observations would test our theoretical understanding of the core-collapse SN phenomenon.

One unequivocal indication of oscillation effects would be the energy-dependent modulation of the survival probability $p(E)$ caused by Earth matter effects [29]. The Earth matter effects can be revealed by wiggles in energy spectra and LENA benefit from a better energy resolution than MEMPHYS in this respect which may be partially compensated by 10 times more statistics [30]. The Earth effect would show up in the $\bar{\nu}_e$ channel for the normal mass hierarchy, assuming that θ_{13} is large (Table 7). Another possibility to establish the presence of Earth effects is to use the signal from two detectors if one of them sees the SN shadowed by the Earth and the other not. A comparison between the signal normalization in the two detectors might reveal Earth effects [31]. The shock wave propagation can influence the Earth matter effect, producing a delayed effect 5 – 7 s after the core-bounce, in some particular situations [32] (See Tab. 7).

Exploiting these three experimental signatures, by the joint efforts of the complementarity SN neutrino detection in MEMPHYS, LENA, and GLACIER it would be possible to extract valuable information on the neutrino mass hierarchy and to put a bound on θ_{13} , as shown in Tab. 7.

Other interesting ideas has been also studied in literature, ranging from the pointing of a SN by neutrinos [33], an early alert for SN observatory exploiting the neutrino signal [34], and the detection of neutrinos from the last phases of a burning star [35].

Up to now, we have investigated SN in our Galaxy, but the calculated rate of supernova explosions within a distance of 10 Mpc is about 1 per year. Although the number of events from a single explosion at such large distances would be small, the signal could be separated from the background with the request to observe at least two events within a time window comparable to the neutrino emission time-scale (~ 10 sec), together with the full energy and time distribution of the events [36]. In a MEMPHYS-type detector, with at least two neutrinos observed, a supernova could be identified without optical confirmation, so that the start of the light curve could be forecasted by a few hours, along with a short list of probable host galaxies. This would also allow the detection of supernovae which are either heavily obscured by dust or are optically dark due to prompt black hole formation.

Mass Hierarchy	$\sin^2 \theta_{13}$	ν_e neutronization peak	Shock wave	Earth effect
Normal	$\gtrsim 10^{-3}$	Absent	ν_e	$\bar{\nu}_e$ ν_e (delayed)
Inverted	$\gtrsim 10^{-3}$	Present	$\bar{\nu}_e$	ν_e $\bar{\nu}_e$ (delayed)
Any	$\lesssim 10^{-5}$	Present	-	both $\bar{\nu}_e$ ν_e

Table 7: Summary of the neutrino properties effect on ν_e and $\bar{\nu}_e$ signals.

3.2.3 Diffuse Supernova Neutrino Background

A galactic Supernova explosion will be a spectacular source of neutrinos, so that a variety of neutrino and SN properties could be determined. However, only one such explosion is expected in 20 to 100 years. Alternatively, it has been suggested that we might detect the cumulative neutrino flux from all the past SN in the Universe, the so called Diffuse Supernova Neutrino Background (DSNB) ¹. In particular, there is an energy window around 20 – 40 MeV where the DSNB signal can emerge above other sources, so that proposed detectors may measure this flux after some years of exposure times.

The DSNB signal, although weak, is not only “guaranteed”, but can also probe different physics from a galactic SN, including processes which occure on cosmological scales in time or space. This makes them complementary to electromagnetic radiation which is much easier to detect, but also much easier to be absorbed or scattered on its way.

For instance, the DSNB signal is sensitive to the evolution of the SN rate, which is closely related to the star formation rate [37, 38]. Additionally, neutrino decay scenarios with cosmological lifetimes could be analyzed and constrained [39], as proposed in [40].

An upper limit on the DSNB flux has been set by the Super-Kamiokande experiment [41]

$$\phi_{\bar{\nu}_e}^{DSNB} < 1.2 \text{ cm}^{-2} \text{ s}^{-1} \quad (E_\nu > 19.3 \text{ MeV}) \quad (7)$$

However most of the estimates are below this limit and therefore DSNB detection appears to be feasible only with the large detector foreseen, through $\bar{\nu}_e$ inverse beta decay in MEMPHYS and LENA detectors and through $\nu_e + {}^{40}\text{Ar} \rightarrow e^- + {}^{40}\text{K}^*$ (and the associated gamma cascade) in GLACIER.

¹We prefer the "Diffuse" rather the "Relic" word to not confuse with the primordial neutrinos produced one second after the Big Bang.

Typical estimates for DSNB fluxes (see for example [38]) predict an event rate of the order of $(0.1 \div 0.5) \text{ cm}^{-2} \text{ s}^{-1} \text{ MeV}^{-1}$ for energies above 20 MeV.

The DSNB signal energy window is constrained from above by the atmospheric neutrinos and from below by either the nuclear reactor $\bar{\nu}_e$ (I), the spallation production unstable radionuclei by cosmic ray muons (II), the decay of "invisible" muon into electron (III), and solar ν_e neutrinos (IV). The three detectors are affected differently these backgrounds. Namely, MEMPHYS filled with pure water is mainly affected by type III due to the fact that the muons may have not enough energy to produce Čerenkov light, while LENA takes benefit from the delayed neutron capture in $\bar{\nu}_e + p \rightarrow n + e^+$, so it is mainly affected by type I which impose to choose an underground site far from nuclear plants, and GLACIER looking at ν_e is mainly affected by type IV. As pointed out in [26], with addition of Gadolinium [7] the detection of the captured neutron releasing 8 MeV gamma after of the order of 20 μs (10 times faster than in pure water), would give the possibility to reject neutrinos other than $\bar{\nu}_e$ that is to say not only the "invisible" muon (type III) but also the spallation background (type II).

The expected rates of signal and background are presented in Tab. 8. As an

Interaction	Exposure	Energy Window	Signal/Bkgd
MEMPHYS + 0.2% Gd (at Kamioka)			
$\bar{\nu}_e + p \rightarrow n + e^+$	1 Mt.y	[15 – 30] MeV	(60-150)/65
$n + Gd \rightarrow \gamma$	2 yrs		
(8 MeV, 20 μs)			
LENA at Pyhäsalmi			
$\bar{\nu}_e + p \rightarrow n + e^+$	0.4 Mt.y	[9.5 – 30] MeV	(40-260)/20
$n + p \rightarrow d + \gamma$	10 yrs		
(2 MeV, 200 μs)			
GLACIER			
$\nu_e + {}^{40}\text{Ar} \rightarrow e^- + {}^{40}\text{K}^*$	0.5 Mt.y	[16 – 40] MeV	(?-60)/30
	5 yrs		

Table 8: DSNB expected rates. The larger numbers are computed with the present limit on the flux by SuperKamiokande collaboration. The lower numbers are computed for typical models. The background coming from reator plants have been computed for specific locations for MEMPHYS and LENA. For MEMPHYS one has been using the SuperKamiokande background scaled by the exposure. More studies are needed to estimate the background at the new Fréjus laboratory.

example of energy spectra, for the MEMPHYS detector, the results are shown in Fig. 9: the signal could be observed with a statistical significance of about 2 standard deviations after 10 years. The spectra of the two backgrounds were taken from the Super-Kamiokande estimates and rescaled to a fiducial mass of 440 kton of water, while the expected signal was computed according to the model called LL in [38].

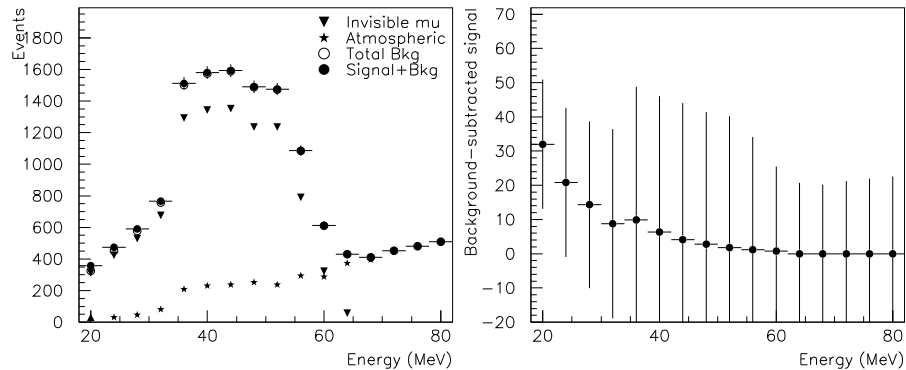


Figure 9: *Supernova relic neutrino signal and backgrounds (left) and subtracted signal with statistical errors (right) in a 440 kt water cherenkov detector with a 10 years exposure. The selection efficiencies of SK were assumed; the efficiency change at 34 MeV is due to the spallation cut.*

3.3 Solar neutrinos

Version 0 from J.E.C 3/3/06
update by A. Bueno 23/3/06

In the past years Water Cherenkov detectors have measured the high energy tail ($E > 5$ MeV) of the solar ^8B neutrino flux using electron-neutrino elastic scattering [42]. Since such detectors could record the time of an interaction and reconstruct the energy and direction of the recoiling electron, unique information of the spectrum and time variation of the solar neutrino flux was extracted. This provided further insights into the “solar neutrino problem”, the deficit of the neutrino flux (measured by several experiments) with respect to the flux expected by the standard solar models. It also constrained the neutrino flavor oscillation solutions in a fairly model-independent way.

With MEMPHYS, Super-Kamiokande’s measurements obtained from 1258 days of data could be repeated in about half a year (the seasonal flux variation measurement requires of course a full year). In particular, a first measurement of the flux of the rare “hep” neutrinos may be possible. Elastic neutrino-electron scattering is strongly forward peaked. To separate the solar neutrino signal from the isotropic background events (mainly due to low radioactivity), this directional correlation is exploited. Angular resolution is limited by multiple scattering. The reconstruction algorithm first reconstructs the vertex from the PMT times and then the direction assuming a single Cherenkov cone originating from the reconstructed vertex. Recon-

structuring 7 MeV events in MEMPHYS seems not to be a problem and decreasing the threshold would imply serious care of the detector radioactivity level as well as the laboratory environment as air free of radon (cf. SNO Laboratory). **To be completed...**

With LENA, one would in principle get a large amount of neutrinos from ${}^7\text{Be}$ ($\sim 5.4 \cdot 10^3/\text{day}$) to test small flux fluctuation in time over the general seasonal variation. The *pep* neutrinos as well as the CNO cycle induced neutrinos are expected also to be recorded at a rate of 300/day, this would constraint the CNO contribution to the solar energy release and to better understand the global solar neutrino luminosity. However, the observation of such solar neutrinos in these detectors, through i.e elastic scattering, is not a simple task, since neutrino events cannot be separated from the background, and it can be accomplished only if the detector contamination will be kept very low [44]. Moreover, only mono-energetic sources as such mentioned can be detected, taking advantage of the Compton-like shoulder edge produced in the event spectrum. Recently, it has been investigated the possibility to register $\sim 1000/\text{year}$ ${}^8\text{B}$ solar neutrinos by means of the charged current interaction with the ${}^{13}\text{C}$ nuclei naturally contained in organic scintillators. Even, if the event signal does not keep the directionality of the neutrino, it can be separated from the background by exploiting the time and space coincidence with the subsequent decay of the produced ${}^{13}\text{N}$ nuclei (remaining background of about 60/year corresponding to a reduction factor of $\sim 3 \cdot 10^{-4}$.) [43]. The propose LENA location in Pyhäsalmi (~ 4000 m.w.e.) means that the cosmogenic background will be sufficiently low for the proposed measure. Notice that Fréjus location would be also good in this respect (~ 4800 m.w.e.). The radioactivity of the detector would have to be kept very low (10^{-17} g/g level U-Th) as in the KamLAND detector. **To be completed...**

The solar neutrinos in GLACIER can be registered through the elastic scattering $\nu_x + e^- \rightarrow \nu_x + e^-$ (ES) and the absorption reaction $\nu_e + {}^{40}\text{Ar} \rightarrow e^- + {}^{40}\text{K}^*$ (ABS) followed by γ s emission. Even if these reactions have low threshold (e.g 1.5 MeV for the second one), one expects to operate in practice with a threshold set at 5 MeV on the primary electron kinetic energy to reject background from neutron capture followed by gamma ray emission which constitute the main background in some underground laboratory [45] as for the LNGS (Italy). These neutrons are induced by the spontaneous fission of the cavern rock (note that in case of a salt mine this background may be significantly reduced).

The expected raw event rate is 330,000/year (66% from ABS, 25% from ES and 9% from neutron background induced events) assuming the above mentioned threshold on the final electron energy. Then, applying further offline cuts to purify separately the ES sample and the ABS sample, one gets the rates shown on table 9.

A possible way to combine the ES and the ABS channels similar to the NC/CC

	Events/year
Elastic channel ($E \geq 5$ MeV)	45,300
Neutron bkgd	1,400
Absorption events contamination	1,100
Absorption channel (Gamow-Teller transition)	101,700
Absorption channel (Fermi transition)	59,900
Neutron bkgd	5,500
Elastic events contamination	1,700

Table 9: Number of events expected in GLACIER per year, compared with the computed background (no oscillation) in the Gran Sasso Laboratory (Italy) rock radioactivity condition (i.e. $0.32 \cdot 10^{-6} \text{ n cm}^{-2} \text{ s}^{-1} (> 2.5 \text{ MeV})$). The Absorption channel have been split into the contributions of events from Fermi transition and from Gamow-Teller transition of the ^{40}Ar to the different ^{40}K excited levels and that can be separated using the emitted gamma energy and multiplicity

flux ratio measured by SNO collaboration [46], is to compute the following ratio:

$$R = \frac{N^{ES}/N_0^{ES}}{\frac{1}{2} \left(N^{ABS-GT}/N_0^{ABS-GT} + N^{ABS-F}/N_0^{ABS-F} \right)} \quad (8)$$

where the numbers of expected events without neutrino oscillations are labeled with a 0). This double ratio has the following advantages: first it is independent of the ^8B total neutrino flux, predicted by different solar models, and second it is free of experimental threshold energy bias and of the adopted cross-sections for the different channels. With the present fit to solar and KamLAND data (see sec. 3.5), one expects a value of $R = 1.30 \pm 0.01$ after one year of data taking with GLACIER. The quoted error for R only takes into account statistics.

3.4 Geo neutrinos

Version 0 by JEC 2/3/06

The total power dissipated from the Earth (heat flow) has been measured with thermal techniques to be 44.2 ± 1.0 TW. Despite this small quoted error, a more recent evaluation of the same data (assuming much lower hydrothermal heat flow near mid-ocean ridges) has led to a lower figure of 31 ± 1 TW. On the basis of studies of chondritic meteorites the calculated radiogenic power is thought to be 19 TW (about half of the total power), 84% of which is produced by ^{238}U and ^{232}Th decay which in turn produce $\bar{\nu}_e$ by β decays. It is then of prime importance to measure the $\bar{\nu}_e$ flux coming from the Earth to get geophysical information, with possible applications in the interpretation of the geomagnetism.

The KamLAND collaboration has recently reported the first observation of the geo-neutrinos [47]. The events are identified by the time and distance coincidence between the prompt e^+ and the delayed (200 μs) neutron capture produced by $\bar{\nu}_e + p \rightarrow n + e^+$ and emitting a 2.2 MeV photons. The energy window to look at the geo-neutrino events is [1.7, 3.4] MeV: the lower bound corresponds to the reaction threshold while the upper bound is constraints by the nuclear reactor induced background events. The measured rate in the 1 kT liquid scintillator detector located at Kamioka (Japan) is 25_{-18}^{+19} for a total background of 127 ± 13 events. The background is composed by 2/3 of $\bar{\nu}_e$ from the nuclear reactors in Japan and Korea² and 1/3 of events coming from neutrons of 7.3 MeV produced in $^{13}\text{C}(\alpha, n)^{16}\text{O}$ reactions and captured as in the inverse beta decay reaction. The α particles come from the ^{210}Po decays daughter of the ^{222}Rn of natural radioactivity origin. The measured geo-neutrino events can be converted in a rate of $5.1_{-3.6}^{+3.9} 10^{-31} \bar{\nu}_e$ per target proton per year corresponding to a mean flux of $5.7 10^6 \text{ cm}^{-2} \text{ s}^{-1}$, or this can be transformed into a 99% CL upper bound of $1.45 10^{-30} \bar{\nu}_e$ per target proton per year ($1.62 10^7 \text{ cm}^{-2} \text{ s}^{-1}$ and 60 TW for the radiogenic power).

The KamLAND result is at $\sim 2\sigma$ level and needs to be confirmed by much more and cleaner statistics. It is expected to register 1500 events per year in the LENA detector if one takes the mean value of the rate measured by KamLAND. But in the same times the background may be reduced. The reactor neutrino background may be lowered by choosing a different location far from nuclear plants as at Pyhäsalmi mine (Finland), where one expects a factor ~ 20 reduction (**To be confirmed by LENA**). The α induced background may also be lowered requiring R&D to reduce the natural radioactivity of the detector (the present level of U-Th in KamLAND is 10^{-17} g/g) as well as the Radon content of the environment.

In MEMPHYS, one expects 10 times more geo-neutrino events but this would imply to decrease the trigger threshold to 2 MeV which seems challenging with respect to the present SuperKamiokande threshold set to 4.6 MeV due to high level of raw trigger rate 120 Hz and increasing by a factor 10 each times the trigger is lowered by 1 MeV [48]. This trigger rate is driven by a number of factors as γ s from the rock surrounding the detector, radioactive decay in the PMT glass itself and Radon contamination in the water. So, it is a general interest to study in details the possibility to tackle the natural radioactivity of the detectors and their environment.

To be confirmed by MEMPHYS

In GLACIER the $\bar{\nu}_e + ^{40}\text{Ar} \rightarrow e^+ + ^{40}\text{Cl}^*$ has a threshold of 7.5 MeV too high for geo-neutrino detection.

3.5 Neutrinos from reactors

Version 0 by JEC 2/3/06

²These events have been used by KamLAND to confirm and measure precisely the Solar driven neutrino oscillation parameters 3.6.

updated by A. Bueno 23/3/06

It has been shown in sections 3.2 and 3.4 that $\bar{\nu}_e$ originated from nuclear reactors can be a serious background for diffuse Supernova and geo-neutrino detections. But, a background on one side can be also turned to useful foreground on an other side. In particular, the KamLand 1 kT liquid scintillator detector located at Kamioka had measured the flux of 53 Japanese power reactors delivering 701Joule/cm² [49]. The event rate of 365.2 ± 23.7 above 2.6 MeV in 766 ton.y exposure from this nuclear power reactors was expected. The observed rate was 258 events with a total of background of 17.8 ± 7.3 . The clear deficit interpreted in terms of neutrino oscillation leads to the measurement of θ_{12} , the neutrino 1-2 family mixing angle ($\sin^2 \theta_{12} = 0.31^{+0.02}_{-0.03}$) as well as the mass squared difference $\Delta m_{12}^2 = 7.9 \pm 0.3 \cdot 10^{-5} \text{eV}^2$ (error quoted at 1 σ).

The area of precise measurement is now under investigation. Running KamLAND for 2-3 more years would gain 30% (4%) reduction in the spread of Δm_{12}^2 (θ_{12}), it has been shown that using Water Čerenkov loaded with Gadolinium to increase by a factor 10 the neutron capture [50] one can expect 80% (34%) reduction of the spread of Δm_{12}^2 (θ_{12}) in 110 kT.y exposure at Kamioka (using SuperKamiokande).

Investigation of what could be expected using MEMPHYS loaded with Gadolinium is under investigation: waiting for the Th. Schwetz and S. Petcov letter.

There have been no studies concerning the detection of reactor neutrinos with LAr TPC. I do not know whether this section is relevant or not, given the small amount of information we are able to give.

To be completed by LENA.

3.6 Neutrino oscillation physics

Version 0 C&P from MEMPHYS document to CERN Strategic Group

updated by A. Bueno 23/3/06

3.6.1 with the CERN-SPL SuperBeam

In the initial CERN-SPL SuperBeam project [51, 52, 53, 54, 55] the planned 4MW SPL (Superconducting Proton Linac) would deliver a 2.2 GeV/c proton beam sent on a Hg target to generate an intense π^+ (π^-) beam focused by a suitable magnetic horn in a short decay tunnel. As a result, an intense ν_μ beam is produced mainly via the π -decay, $\pi^+ \rightarrow \nu_\mu \mu^+$ providing a flux $\phi \sim 3.6 \cdot 10^{11} \nu_\mu / \text{year} / \text{m}^2$ at 130 Km of distance, and an average energy of 0.27 GeV. The ν_e contamination from K is suppressed by threshold effects and amounts to 0.4%. The use of a near and far detector (the latter 130 km away at Fréjus [56], see Sec. ??) will allow for both ν_μ -disappearance and $\nu_\mu \rightarrow \nu_e$ appearance studies. The physics potential of the 2.2 GeV SPL SuperBeam (SPL-SB) with a water Čerenkov far detector with a fiducial mass of 440 kton, has been extensively studied [52].

New developments show that the potential of the SPL-SB potential could be improved by rising the SPL energy to 3.5 GeV [57], to produce more copious secondary mesons and to focus them more efficiently. This increase in energy is made possible by using state of the art RF cavities instead of the previously foreseen LEP cavities [58].

The focusing system (magnetic horns) originally optimized in the context of a Neutrino Factory [59, 60] has been redesigned considering the specific requirements of a Super Beam. The most important points are that the phase spaces that are covered by the two types of horns are different, and that for a Super Beam the pions to be focused should have an energy of the order of 800 MeV to get a mean neutrino energy of 300 MeV. The increase in kaon production rate, giving higher ν_e contamination, has been taken into account, and should be refined using HARP results [61].

In this upgraded configuration, the neutrino flux is increased by a factor ~ 3 with respect to the 2.2 GeV configuration, and the number of expected ν_μ charged currents is about 95 per kton \cdot yr in MEMPHYS.

A sensitivity $\sin^2 2\theta_{13} < 0.8 \cdot 10^{-3}$ is obtained in a 2 years ν_μ plus 8 year $\bar{\nu}_\mu$ run (for $\delta = 0$, intrinsic degeneracy accounted for, sign and octant degeneracies not accounted for), allowing for a discovery of CP violation (at 3σ level) for $\delta \geq 60^\circ$ for $\theta_{13} = 1.2^\circ$, and improving to $\delta \geq 20^\circ$ for $\theta_{13} \geq 4^\circ$ [62, 63]. These performances are shown in Fig. 12, they are found equivalent to Hyperkamioka. These limits have been obtained first using realistic simulations based on Superkamiokande performances (Background level, signal efficiencies, and associated systematics at the level of 2%), and more recently confirmed using GLoBES [64].

Let us conclude this section by mentioning that further studies of the SPL super-beam will take place inside the Technical Design Study to be submitted to Europe by the neutrino factory community towards the end of 2006.

3.6.2 with the CERN BetaBeams

BetaBeams have been proposed by P. Zucchelli in 2001 [65]. The idea is to generate pure, well collimated and intense ν_e ($\bar{\nu}_e$) beams by producing, collecting, accelerating radioactive ions and storing them in a decay ring in 10 ns long bunches, to suppress the atmospheric neutrino backgrounds. The resulting BetaBeam spectra can be easily computed knowing the beta decay spectrum of the parent ion and the Lorentz boost factor γ , and these beams are virtually background free from other flavors. The best ion candidates so far are ^{18}Ne and ^6He for ν_e and $\bar{\nu}_e$ respectively. The schematic layout of a Beta Beam is shown in figure 11. It consists of three parts :

1. A low energy part, where a small fraction (lower than 10%) of the protons accelerated by the SPL are shot on specific target to produce ^{18}Ne or ^6He ; these ions are then collected by an ECR source of new generation [66] which

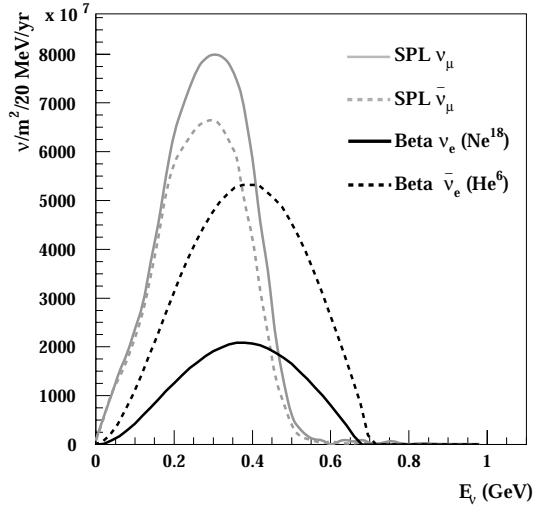


Figure 10: *Neutrino flux of β -Beam ($\gamma = 100$) and CERN-SPL SuperBeam, 3.5 GeV, at 130 Km of distance.*

delivers ion bunches with 100 keV energy, then accelerated in a LINAC up to 100 MeV/u. This part could be shared with nuclear physicists involved in the EURISOL project [67].

2. The acceleration to the final energy uses a rapid cycling cyclotron (labelled PSB) which further accelerates and bunches the ions before sending them to the PS and the SPS, where they reach their final energy (γ around 100). In this process, 16 bunches (150 ns long) in the booster are transformed into 4 bunches (10 ns long) in the SPS.
3. Ions of the required energy are then stored in a decay ring, with 2500 m long straight sections for a total length of 7000 m, so that 36% of the decays give a strongly collimated and ultra pure neutrino beam aimed at the Fréjus detector.

A baseline study for the betabeam has been initiated at CERN, and is now going on within the european FP6 design study for EURISOL. A specific task is devoted to the study of the high energy part (last 2 items above). A complete conceptual design for the decay ring has already been performed. The injection in the ring uses the asymmetric merging scheme, validated by experimental tests at CERN. The actual performances of the new ECR sources will also be studied with prototypes in the framework of the EURISOL design study.

The potential of such betabeams sent to MEMPHYS has been studied in the context of the baseline scenario, using reference fluxes of $5.8 \cdot 10^{18}$ ${}^6\text{He}$ useful decays/year and $2.2 \cdot 10^{18}$ ${}^{18}\text{Ne}$ decays/year, corresponding to a reasonable estimate by experts in the field of the ultimately achievable fluxes .

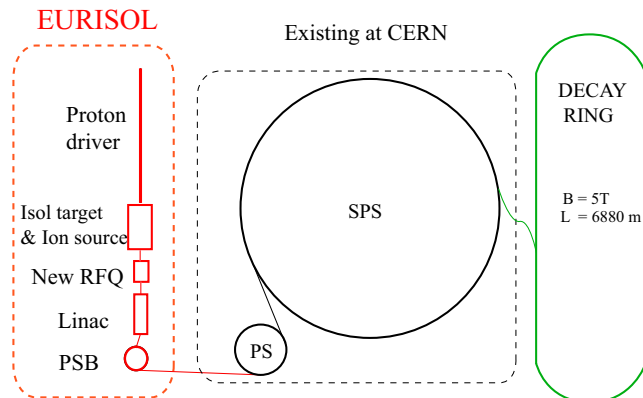


Figure 11: A schematic layout of the BetaBeam complex. On the left, the low energy part is largely similar to the EURISOL project [67]. The central part (PS and SPS) uses existing facilities. On the right, the decay ring has to be built.

First oscillation physics studies [69, 70, 71, 72] used $\gamma_{\text{He}} = 60$ and $\gamma_{\text{Ne}} = 100$. But it was soon realized that the optimal values were actually $\gamma = 100$ for both species, and the corresponding performances are shown in figure 12, exhibiting a strong improvement over SPL superbeam performances, extending the range of sensitivity for θ_{13} down to 0.4 degree, and improving CP violation sensitivity at lower values of θ_{13} .

To conclude this section, let us mention a very recent development of the Beta Beam concept leading to the possibility to have monochromatic, single flavor neutrino beams by using ions decaying through the electron capture process [73, 74]. A suitable ion candidate exists: ^{150}Dy , whose performances have been already delineated [73]. Such beams would in particular be perfect to precisely measure neutrino cross sections in a near detector with the possibility of an energy scan by varying the γ value of the ions.

3.6.3 combining SPL Super Beam and Beta Beam

Since betabeams use only a small fraction of the protons available from the SPL, both beta beam and superbeam can be run at the same time. The combination of superbeam and betabeam results further improves the sensitivity on θ_{13} and δ , as shown on figure 12. It is better in all cases than Hyperkamioka sensitivity, except maybe for very large values of θ_{13} above 6° . The sensitivity on CP violation is even better than that of a neutrino factory for θ_{13} above 1.7° (but neutrino factories are still a factor 3 better for θ_{13} sensitivity). This combination of super and betabeams offers other advantages, since the same parameters θ_{13} and δ_{CP} may be measured in many different ways, using 2 pairs of CP related channels, 2 pairs of T related

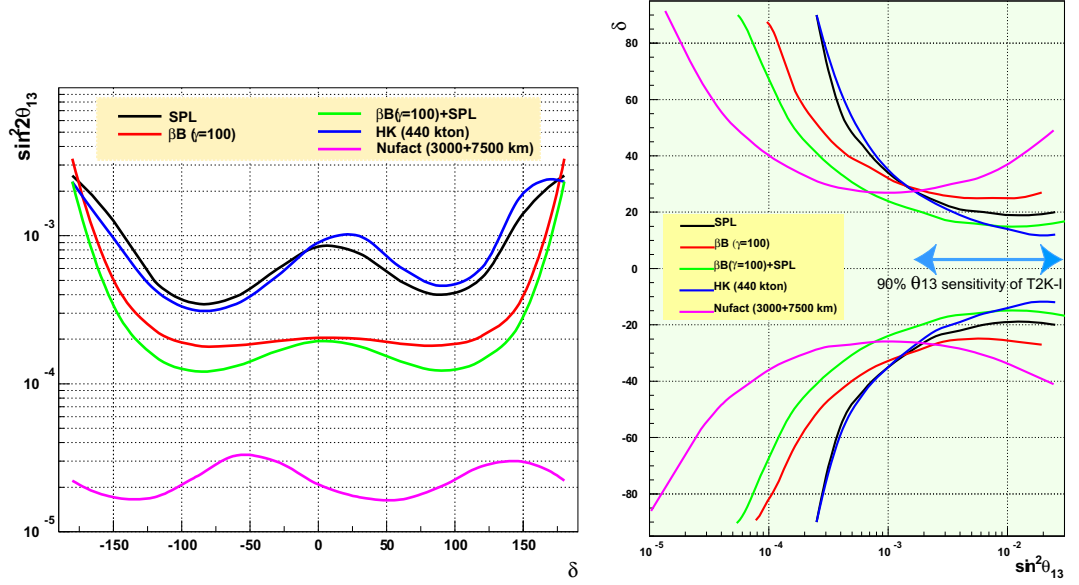


Figure 12: *LEFT*: θ_{13} 90% C.L. sensitivity as function of δ_{CP} for $\Delta m_{23}^2 = 2.5 \cdot 10^{-3} \text{eV}^2$, $\text{sign}(\Delta m_{23}^2) = 1$, 2% systematic errors. SPL-SB sensitivities have been computed for a 2 year ν_μ + 8 year $\bar{\nu}_\mu$ run, βB ($\gamma = 100$) for a 5 year ν_e + 5 year $\bar{\nu}_e$ run, 200 MeV energy bins for both beams. The combination of SPL-SB and βB is also shown. HK and NuFACT curves are adapted from [68]: HK curves corresponds to Hyperkamioka with the same fiducial mass, running time and systematics as MEMPHYS, using the 4MW beam from JAERI. The NuFACT curve corresponds to 5 year runs for each polarity, two 50kton iron detectors located at 3000 and 7000 km receiving neutrinos from 10^{21} useful 50 GeV muon decays per year, detector systematics set at 2%, matter profile uncertainty set at 5%, energy threshold set at 4 GeV. *RIGHT*: δ_{CP} discovery potential at 3σ computed for the same conditions.

channels, and 2 pairs of CPT related channels which should all give coherent results. In this way the estimates of the systematic errors, different for each beam, will be experimentally cross-checked. And, needless to say, the unoscillated data for a given beam will give a large sample of events corresponding to the small searched-for signal with the other beam, adding more handles on the understanding of the detector response.

Finally, a common criticism made to projects like MEMPHYS using sub-GeV beams is that they get no sensitivity on the mass hierarchy, contrary to other projects with higher energy beams. However, a recent study [75] has shown that low energy Super Beam and Beta Beam can profit of atmospheric neutrino oscillations, detected with large statistics in a megaton scale water Čerenkov detector, to solve degeneracies and measure $\text{sign}(\Delta m_{23}^2)$.

3.6.4 comparison with other projects

Before the advent of megaton class detectors receiving neutrino from a Super Beam and/or Beta Beam, several beam experiments (MINOS, OPERA, T2K, NoVA) and reactor experiments (such as Double-CHOOZ) will have improved our knowledge on θ_{13} .

If θ_{13} is found by these experiments, it will be "big" (above 4 degrees), and megaton detectors will be the perfect tool to study CP violation, with no need for a neutrino factory. If on the contrary, only an upper limit around 2 to 3 degrees is given on θ_{13} , one might consider an alternative between a staged strategy, starting with megaton detectors, to explore θ_{13} down to 0.5 degree and start a rich program of non oscillation physics, eventually followed by a neutrino factory if θ_{13} is not found; or a more aggressive strategy, aiming directly at neutrino factories to explore θ_{13} down to 0.3 degree, but with no guarantee of success; in the latter case, the non-oscillation physics (proton decay, supernovae) is lost, but would be replaced by precision muon physics (which has to be assessed and compared with other projects in this field).

There is no doubt that a neutrino factory has a bigger potential than megaton detectors for very low values of θ_{13} (below 2 degrees), and the only competition in that case could come from so-called high energy beta-beams. An abundant literature has been published on this subject (see [76, 77, 78, 79, 80, 81]), but most authors have taken as granted that the neutrino fluxes from betabeams could be kept the same at higher energies, which is far from evident [82] and implies a lot of R&D on the required accelerators and storage rings before a useful comparison can be made with neutrino factories.

Presently, the only pertinent comparison is between the several megaton projects, namely UNO, Hyperkamiokande and MEMPHYS, or their variants using liquid argon technology (such as FLARE in the USA, GLACIER in Europe). In this document, we have shown a comparison between Hyperkamiokande and MEMPHYS, showing a definite advantage for the latter, due to the betabeam. However, recent variants

of Hyperkamiokande using a second detector in Korea would have to be considered. UNO, for the time being, refers to a study of a very long baseline (2500 km) neutrino wide band superbeam produced at Brookhaven, which gives a disappointing sensitivity on θ_{13} at the level of 4 degrees (this is due to the fact that this multiGeV beam leads to high π^0 backgrounds in a water Čerenkov detector, as explained before). Liquid argon detector performances have to be studied, but they will probably suffer from their lower mass for the lower limit on θ_{13} , while a better visibility of event topologies would probably help for high values of θ_{13} , when statistics become important and systematics dominate; all this has still to be carefully quantified.

Let us mention that a unified way to compare different projects has been made available to the community, this is the GLoBES package [64]. Figure 12 in this document was actually produced using GLoBES, and some of us are actively pursuing GLoBES-based comparisons in the framework of the International Scoping Study (ISS), with results expected by mid-2006. They will also address the best way to solve problems related to the degeneracies on parameter estimates due to the sign of Δm_{23}^2 , the quadrant ambiguity on θ_{23} , as well as intrinsic (analytic) ambiguities (In the present document, we have supposed θ_{23} equal to 45° , and the absence of matter effects at low energies make the results insensitive to the mass hierarchy). But the main point is to feed GLoBES with realistic estimates of the expected performances of the different projects, in terms of background rejection, signal efficiencies and the various related systematic uncertainties. A coordinated effort to get realistic numbers for the different projects will be, if successful, an important achievement of the ISS initiative.

3.6.5 Neutrino Factory LAr detector

In order to fully address the oscillation processes at a neutrino factory, a detector should be capable of identifying and measuring all three charged lepton flavors produced in charged current interactions *and* of measuring their charges to discriminate the incoming neutrino helicity. This is an experimentally challenging task, given the required detector mass for long-baseline experiments.

The GLACIER concept offers a high-granularity, excellent-calorimetry non-magnetized target-detector, which provides a background-free identification of electron neutrino charged current and a kinematical selection of tau neutrino charged current interactions. We can assume that charge discrimination is available for muons reaching an external magnetized-Fe spectrometer. Another interesting and extremely challenging possibility would consist on magnetizing the whole liquid argon volume [83]. This set-up allows the clean classification of events into electron, right-sign muon, wrong-sign muon and no-lepton categories. In addition, high granularity permits a clean detection of quasi-elastic events, which by detecting the final state proton, provide a selection of the neutrino electron helicity without the need of an electron charge measurement.

Table 10 summarizes the expected rates for GLACIER and 10^{20} muon decays (expected 1 year of operation) at a neutrino factory with stored muons having an energy of 30 GeV [84]. N_{tot} is the total number of events and N_{qe} is the number of quasi-elastic events.

Event rates for various baselines								
			L=732 km		L=2900 km		L=7400 km	
			N_{tot}	N_{qe}	N_{tot}	N_{qe}	N_{tot}	N_{qe}
10^{20} decays	μ^-	ν_μ CC	2260000	90400	144000	5760	22700	900
		ν_μ NC	673000	—	41200	—	6800	—
		$\bar{\nu}_e$ CC	871000	34800	55300	2200	8750	350
		$\bar{\nu}_e$ NC	302000	—	19900	—	3000	—
10^{20} decays	μ^+	$\bar{\nu}_\mu$ CC	1010000	40400	63800	2550	10000	400
		$\bar{\nu}_\mu$ NC	353000	—	22400	—	3500	—
		ν_e CC	1970000	78800	129000	5160	19800	800
		ν_e NC	579000	—	36700	—	5800	—

Table 10: Expected events rates for the GLACIER detector in case no oscillations occur for 10^{20} muon decays. We assume $E_\mu=30$ GeV. N_{tot} is the total number of events and N_{qe} is the number of quasi-elastic events.

Figure 13 shows the expected sensitivity in the measurement of the mixing angle between the first and the third family for a baseline of 7400 km. The maximal sensitivity to θ_{13} is achieved for very small background levels, since we are looking in this case for small signals; most of the information is coming from the clean wrong-sign muon class and from quasi-elastic events. On the other hand, if its value is not too small, for a measurement of θ_{13} , the signal/background ratio could be not so crucial, and also the other event classes can contribute to this measurement.

Like for a B-Factory, a ν -Factory should have among its aims the overconstraining of the oscillation pattern, in order to look for unexpected new physics effects. This can be achieved in global fits of the parameters, where the unitarity of the mixing matrix is not strictly assumed. Using a detector able to identify the τ lepton production via kinematic means, it is possible to verify the unitarity in $\nu_\mu \rightarrow \nu_\tau$ and $\nu_e \rightarrow \nu_\tau$ transitions. For this latter, the possibility of a kinematical τ identification for wrong-sign muon events could allow for the first time a clear identification of this type of oscillations.

The study of CP violation in the lepton system is a very fascinating subject and probably, the most ambitious goal of an experiment at a neutrino factory. Matter effect can mimic CP violation; however, a multiparameter fit at the right baseline can allow a simultaneous determination of matter and CP-violating parameters.

To detect CP violation effects, the most favorable choice of neutrino energy E_ν

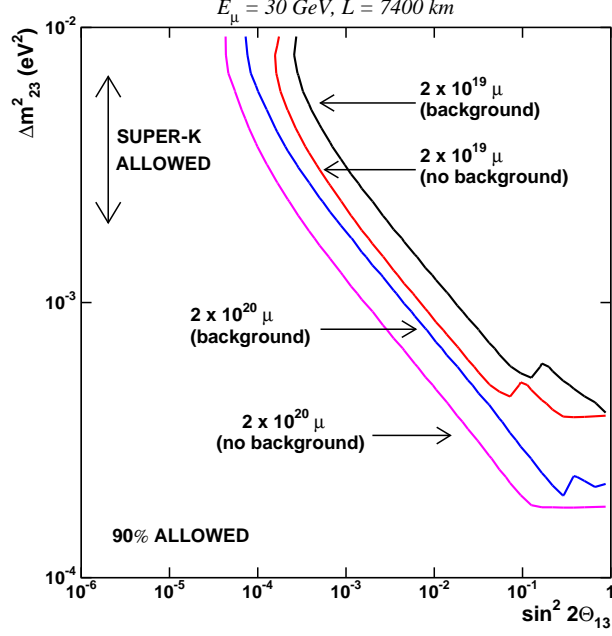


Figure 13: GLACIER sensitivity for θ_{13} .

and baseline L is in the region of the “first maximum”, given by $(L/E_\nu)^{max} \simeq 500$ km/GeV for $|\Delta m_{32}^2| = 2.5 \times 10^{-3}$ eV² [85]. To study oscillations in this region, one has to require that the energy of the “first-maximum” be smaller than the MSW resonance energy: $2\sqrt{2}G_F n_e E_\nu^{max} \lesssim \Delta m_{32}^2 \cos 2\theta_{13}$. This fixes a limit on the baseline $L_{max} \approx 5000$ km beyond which matter effects spoil the sensitivity.

As an example, Fig. 14 shows the sensitivity on the CP violating phase δ for two concrete cases. We have classified the events in the five categories previously mentioned, assuming an electron charge confusion of 0.1%. We have computed the exclusion regions in the $\Delta m_{12}^2 - \delta$ plane fitting the visible energy distributions, provided that the electron detection efficiency is $\sim 20\%$. The excluded regions extend up to values of $|\delta|$ close to π , even when θ_{13} is left free.

3.7 Indirect Search for Dark Matter

Version 0 by AB 23/03/06

WIMPs that constitute the halo of the Milky Way can occasionally interact with massive objects, such as stars or planets. When they scatter off of such an object, they can potentially lose enough energy that they become gravitationally bound and eventually will settle in the center of the celestial body. In particular, WIMPs can be captured by and accumulate in the core of the Sun.

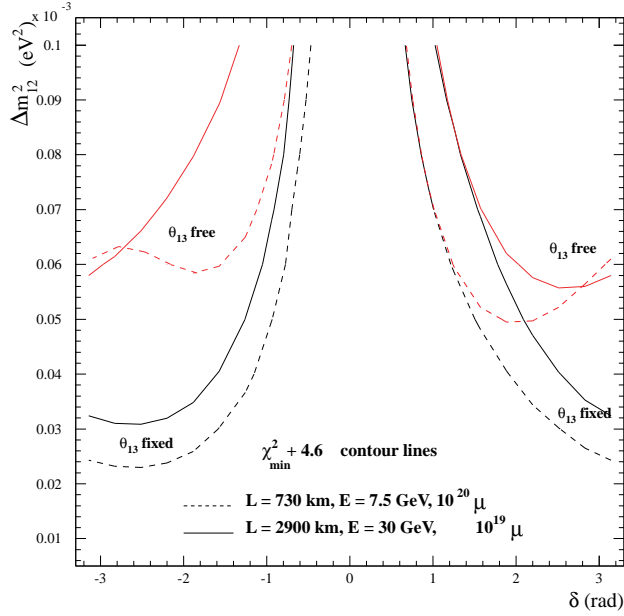


Figure 14: GLACIER 90% C.L. sensitivity on the CP -phase δ as a function of Δm_{21}^2 for the two considered baselines. The reference oscillation parameters are $\Delta m_{32}^2 = 3 \times 10^{-3} \text{ eV}^2$, $\sin^2 \theta_{23} = 0.5$, $\sin^2 \theta_{12} = 0.5$, $\sin^2 2\theta_{13} = 0.05$ and $\delta = 0$. The lower curves are made fixing all parameters to the reference values while for the upper curves θ_{13} is free.

We have assessed, in a model-independent way, the capabilities that GLACIER offers for identifying neutrino signatures coming from the products of WIMP annihilations in the core of the Sun [86]. Signal events will consist of energetic electron (anti)neutrinos coming from the decay of τ leptons and b quarks produced in WIMP annihilation in the core of the Sun. Background contamination from atmospheric neutrinos is expected to be low. We do not consider the possibility of observing neutrinos from WIMPs accumulated in the Earth. Given the smaller mass of the Earth and the fact that only scalar interactions contribute, the capture rates for our planet are not enough to produce, in our experimental set-up, a statistically significant signal.

Our search method takes advantage of the excellent angular reconstruction and superb electron identification capabilities GLACIER offers to look for an excess of energetic electron (anti)neutrinos pointing in the direction of the Sun. The expected signal and background event rates have been evaluated, in a model independent way,

as a function of the WIMP's elastic scatter cross section for a range of masses up to 100 GeV.

The detector discovery potential, i.e. the number of years needed to claim a WIMP signal has been discovered, is shown in Figs 15 and 16. With the assumed set-up and thanks to the low background environment offered by the LAr TPC, a clear WIMP signal would be detected provided the elastic scattering cross section in the Sun is above $\sim 10^{-4}$ pb.

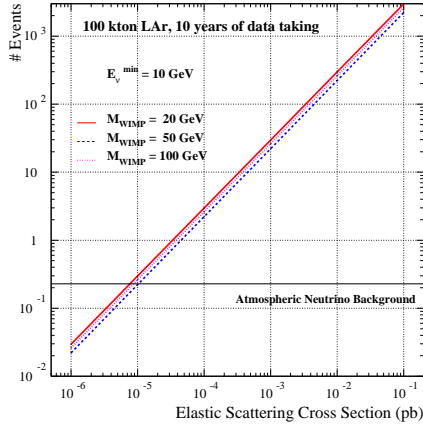


Figure 15: *Expected number of signal and background events as a function of the WIMP elastic scattering production cross section in the Sun, with a cut of 10 GeV on the minimum neutrino energy.*

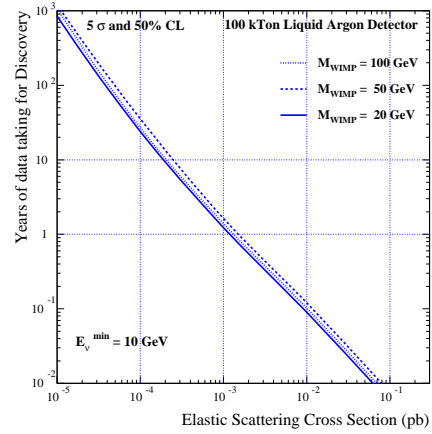


Figure 16: *Minimum number of years required to claim a discovery WIMP signal from the Sun in a 100 kton LAr detector as function of σ_{elastic} for three values of the WIMP mass.*

4 Summary

To be done

Acknowledgments

To be completed: P.F. Perez, A. Mirizzi

References

- [1] A. Rubbia, hep-ph/0402110, hep-ph/0407297; A. Ereditatio, A. Rubbia, hep-ph/0409143.
- [2] S. Amerio *et al.* [ICARUS Collaboration], Nucl. Instrum. Meth. A **527**, 329 (2004).
- [3] A. de Bellefon et al., MEMPHYS: A large scale water Čerenkov detector at Fréjus, Contribution to the CERN strategic committee
- [4] K. Nakamura, "Hyper-Kamiokande: A Next Generation Water Cherenkov Detector", Int. J. Mod. Phys. A18 (2003) 4053-4063
Y. Itow et al., "The JHF-Kamioka Neutrino Project" (arXiv:hep-ex/0106019)
- [5] M. Ishitsuka, T. Kajita, H. Minakata, and H. Nunokawa, Phys. Rev. D72, 033003 (2005), (arXiv:hep-ph/0504026)
- [6] C. K. Jung, Feasibility a Next Generation Underground Water Cherenkov Detector: UNO, Preprint (arXiv:hep-ex/0005046) from the NNN99 Proceedings
- [7] Beacom, J. F. and Vagins, M. R., *Phys. Rev. Lett.* 93 (2004) 171101, arXiv:hep-ph/0309300
- [8] **To be defined**
- [9] P. Nath and P. Fileviez Pérez, "Proton stability in grand unified theories, in strings, and in branes," arXiv:hep-ph/0601023. Submitted to Physics Reports.
- [10] I. Dorsner and P. Fileviez Pérez, "How long could we live?," Phys. Lett. B **625** (2005) 88 [arXiv:hep-ph/0410198].
- [11] H. Georgi and S. L. Glashow, "Unity Of All Elementary Particle Forces," Phys. Rev. Lett. **32** (1974) 438.
- [12] I. Dorsner and P. Fileviez Pérez, "Unification without supersymmetry: Neutrino mass, proton decay and light leptoquarks," Nucl. Phys. B **723** (2005) 53 [arXiv:hep-ph/0504276]; I. Dorsner, P. Fileviez Pérez and R. Gonzalez Felipe, "Phenomenological and cosmological aspects of a minimal GUT scenario," arXiv:hep-ph/0512068.
- [13] D. G. Lee, R. N. Mohapatra, M. K. Parida and M. Rani, "Predictions for proton lifetime in minimal nonsupersymmetric SO(10) models: An update," Phys. Rev. D **51** (1995) 229 [arXiv:hep-ph/9404238].

- [14] H. Murayama and A. Pierce, “Not even decoupling can save minimal supersymmetric SU(5),” *Phys. Rev. D* **65** (2002) 055009 [arXiv:hep-ph/0108104].
 B. Bajc, P. Fileviez Pérez and G. Senjanovic, “Proton decay in minimal supersymmetric SU(5),” *Phys. Rev. D* **66** (2002) 075005 [arXiv:hep-ph/0204311].
 B. Bajc, P. Fileviez Pérez and G. Senjanovic, “Minimal supersymmetric SU(5) theory and proton decay: Where do we stand?,” arXiv:hep-ph/0210374.
 D. Emmanuel-Costa and S. Wiesenfeldt, “Proton decay in a consistent supersymmetric SU(5) GUT model,” *Nucl. Phys. B* **661** (2003) 62 [arXiv:hep-ph/0302272].
- [15] K. S. Babu and R. N. Mohapatra, “Predictive neutrino spectrum in minimal SO(10) grand unification,” *Phys. Rev. Lett.* **70** (1993) 2845 [arXiv:hep-ph/9209215].
 C. S. Aulakh, B. Bajc, A. Melfo, G. Senjanovic and F. Vissani, “The minimal supersymmetric grand unified theory,” *Phys. Lett. B* **588** (2004) 196 [arXiv:hep-ph/0306242].
 T. Fukuyama, A. Ilakovac, T. Kikuchi, S. Meljanac and N. Okada, “Detailed analysis of proton decay rate in the minimal supersymmetric SO(10) model,” *JHEP* **0409** (2004) 052 [arXiv:hep-ph/0406068].
 H. S. Goh, R. N. Mohapatra, S. Nasri and S. P. Ng, “Proton decay in a minimal SUSY SO(10) model for neutrino mixings,” *Phys. Lett. B* **587** (2004) 105 [arXiv:hep-ph/0311330].
- [16] T. Friedmann and E. Witten, “Unification scale, proton decay, and manifolds of G(2) holonomy,” *Adv. Theor. Math. Phys.* **7** (2003) 577 [arXiv:hep-th/0211269].
- [17] A. S. Dighe and A. Y. Smirnov, *Phys. Rev. D* **62**, 033007 (2000).
- [18] K. Hirata *et al.* [KAMIOKANDE-II Collaboration], *Phys. Rev. Lett.* **58**, 1490 (1987).
- [19] K. S. Hirata *et al.*, *Phys. Rev. D* **38**, 448 (1988).
- [20] R. M. Bionta *et al.*, *Phys. Rev. Lett.* **58**, 1494 (1987).
- [21] M. Kachelriess, R. Tomas, R. Buras, H. T. Janka, A. Marek and M. Rampp, *Phys. Rev. D* **71**, 063003 (2005).
- [22] I. Gil-Botella and A. Rubbia, *JCAP* **0408**, 001 (2004) [arXiv:hep-ph/0404151].
- [23] I. Gil-Botella and A. Rubbia, *JCAP* **0310**, 009 (2003)
- [24] R. C. Schirato, G. M. Fuller, (. U. (. LANL), UCSD and LANL), astro-ph/0205390.

- [25] G. L. Fogli, E. Lisi, D. Montanino and A. Mirizzi, *Phys. Rev. D* **68**, 033005 (2003).
- [26] G. L. Fogli, E. Lisi, A. Mirizzi and D. Montanino, *JCAP* **0504**, 002 (2005).
- [27] R. Tomas, M. Kachelriess, G. Raffelt, A. Dighe, H. T. Janka and L. Scheck, *JCAP* **0409**, 015 (2004).
- [28] V. Barger, P. Huber and D. Marfatia, *Phys. Lett. B* **617**, 167 (2005).
- [29] C. Lunardini and A. Yu. Smirnov, *Nucl. Phys. B* **616**, 307 (2001).
- [30] A. S. Dighe, M. T. Keil and G. G. Raffelt, *JCAP* **0306**, 006 (2003).
- [31] A. S. Dighe, M. T. Keil and G. G. Raffelt, *JCAP* **0306**, 005 (2003).
- [32] C. Lunardini and A. Y. Smirnov, *JCAP* **0306**, 009 (2003).
- [33] R. Tomas, D. Semikoz, G. G. Raffelt, M. Kachelriess and A. S. Dighe, *Phys. Rev. D* **68**, 093013 (2003).
- [34] P. Antonioli *et al.*, *New J. Phys.* **6**, 114 (2004).
- [35] A. Odrzywolek, M. Misiaszek and M. Kutschera, *Astropart. Phys.* **21**, 303 (2004).
- [36] Ando, S. and Beacom, J. F. and Yuksel, H., *Phys. Rev. Lett.* 95 (2005) 171101, arXiv:astro-ph/0503321
- [37] M. Fukugita and M. Kawasaki, *Mon. Not. Roy. Astron. Soc.* **340**, L7 (2003).
- [38] S. Ando, *Astrophys. J.* **607**, 20 (2004).
- [39] S. Ando, *Phys. Lett. B* **570**, 11 (2003).
- [40] G. L. Fogli, E. Lisi, A. Mirizzi and D. Montanino, *Phys. Rev. D* **70**, 013001 (2004).
- [41] Malek, M. et al. [Super-Kamiokande Collaboration], *Phys. Rev. Lett.* 90 (2003) 061101, arXiv:hep-ex/0209028
- [42] Smy, M. B. [Super-Kamiokande Collaboration], *Nucl. Phys. Proc. Suppl.* 118 (2003) 25-32, arXiv:hep-ex/0208004
- [43] A. Ianni, D. Montanino and F. L. Villante, *Phys. Lett. B* 627 (2005) 38, arXiv:physics/0506171
- [44] G. Alimonti et al. [Borexino Collaboration], *Astrop. Phys.* 8, 141 (1998); *ibid.*, *Nucl. Instrum. Methods A* 406, 411 (1998)

- [45] P. Arneodo et al. [ICARUS], LNGS-P28/2001, LNGS-EXP 13/89 add. 1/01, ICARUS-TM/2001-03
- [46] B. Aharmim *et al.* [SNO Collaboration], *Phys. Rev. C* 72 (2005) 055502, arXiv:nucl-ex/0502021
- [47] T. Araki et al. [KamLAND], *Nature* 436 (2005) 499-503
- [48] S. Fukuda et al. [SuperKamiokande], *Nucl. Instrum. Methods* A501 (2003) 418-462
- [49] K. Eguchi et al. [KamLAND], *Phys. Rev. Lett.* 90 (2003) 021802; T. Araki et al. , arXiv:hep-ex/0406035
- [50] S. Choubey and S.T. Petcov, *Phys. Lett.* B594 (2004) 333-346
- [51] Autin, B. et al. , CERN-2000-012
- [52] Gomez-Cadenas J. J. et al. , CERN working group on Super Beams (2001), arXiv:hep-ph/0105297
- [53] Blondel A. et al. , *Nucl. Instrum. Methods* A503 (2001) 173-178
- [54] Mezzetto M., *J. Phys. G*29 (2003)1781-1784, arXiv:hep-ex/0302005
- [55] Apollonio M. et al. , arXiv:hep-ph/0210192
- [56] Mosca L., *Nucl. Phys. Proc. Suppl.* 138 (2005) 203-205
- [57] Campagne J.-E. and Cazes A., arXiv:hep-ex/0411062, to appear in *Eur. Phys. J. C* 2005
- [58] Garoby R., *AIP Conf. Proc.* 773 (2005) 239-243
- [59] Gilardoni S. et al. , *AIP Conf. Proc.* 721 (2004) 334-337
- [60] Blondel A. and Donega M. and Gilardoni S., CERN-NUFACT-NOTE-078
- [61] Catanesi M.G. et al. [HARP Collaboration], CERN-SPSC/2001-017 SPSC/P322 May 2001
- [62] Mezzetto M., *Nucl. Phys. Proc. Suppl.* 149 (2005) 179-181
- [63] Campagne J.-E., arXiv:hep-ex/0510029
- [64] Huber P. and Lindner M. and Winter W., *Comput. Phys. Commun.* 167 (2005)195, arXiv:hep-ph/0407333
- [65] Zucchelli P., *Phys. Lett.* B532 (2002) 166-172

- [66] Sortais P., presentations at the Moriond workshop on radioactive beams Les Arcs (France) 2003 ECR technology <http://moriond.in2p3.fr/radio>
- [67] <http://www.ganil.fr/eurisol/>
- [68] Huber P. and Lindner M. and Winter W., Nucl. Phys. B645 (2002)3-48, arXiv:hep-ph/0204352
- [69] Mezzetto M., J. Phys. G29 (2003) 1771-1776, arXiv:hep-ex/0302007
- [70] Bouchez J. and Lindroos M. and Mezzetto M., AIP Conf. Proc. 721 (2004) 37-47, arXiv:hep-ex/0310059
- [71] Mezzetto M., Nucl. Phys. Proc. Suppl. 143 (2005) 309-316, arXiv:hep-ex/0410083
- [72] Donini A. and Fernandez-Martinez E. and Migliozi P. and Rigolin S. and Scotto Lavina L., Nucl. Phys. B710 (2005) 402-424, arXiv:hep-ph/0406132
- [73] Bernabeu J. and Burguet-Castell J. and Espinoza C. and Lindroos M., arXiv:hep-ph/0505054
- [74] Sato J., Phys. Rev. Lett. 95 (2005) 131804, arXiv:hep-ph/0503144
- [75] Huber P. and Maltoni M. and Schwetz Th., Phys. Rev. D71 (2005) 053006, arXiv:hep-ph/0501037
- [76] Burguet-Castell J. and Casper D. and Couce E. and Gomez-Cadenas J. J. and Hernandez P., Nucl. Phys. B725 (2005) 306-326, arXiv:hep-ph/0503021
- [77] Burguet-Castell J. and Casper D. and Gomez-Cadenas J. J. and Hernandez P. and Sanchez F., Nucl. Phys. B695 (2004) 217-240, arXiv:hep-ph/0312068
- [78] Terranova F. and Marotta A. and Migliozi P. and Spinetti M., Eur. Phys. J. C38 (2004) 69-77, arXiv:hep-ph/0405081
- [79] Huber P. and Lindner M. and Rolinec M. and Winter W., arXiv:hep-ph/0506237
- [80] Bruning O. et al. , CERN-LHC-PROJECT-REPORT-626
- [81] Donini A. et al. , arXiv:hep-ph/0511134
- [82] Lindroos M., EURISOL DS/TASK12/TN-05-02 to be published in Nucl. Phys. Proc. Suppl. (2006)
- [83] A. Badertscher, M. Laffranchi, A. Mereaglia, A. Muller and A. Rubbia, Nucl. Instrum. Meth. A **555**, 294 (2005) [arXiv:physics/0505151].

- [84] A. Bueno, M. Campanelli and A. Rubbia, Nucl. Phys. B **589**, 577 (2000) [arXiv:hep-ph/0005007].
- [85] A. Bueno, M. Campanelli, S. Navas-Concha and A. Rubbia, Nucl. Phys. B **631**, 239 (2002) [arXiv:hep-ph/0112297].
- [86] A. Bueno, R. Cid, S. Navas-Concha, D. Hooper and T. J. Weiler, JCAP **0501**, 001 (2005) [arXiv:hep-ph/0410206].